Directly patternable, highly conducting polymers for broad applications in organic electronics

Joung Eun Yoo[a,b], Kwang Seok Lee[b], Andres Garcia[c], Jacob Tarver[a], Enrique D. Gomez[a], Kimberly Baldwin[a], Yangming Sun[b], Hong Meng[d], Thuc-Quyen Nguyen[c], and Yueh-Lin Loo[a,1]

[a]Department of Chemical Engineering, Princeton University, A215 Engineering Quadrangle, Princeton, NJ 08544; [b]Department of Chemical Engineering, University of Texas at Austin, 1 University Station C0400, Austin, TX 78712; [c]Department of Chemistry and Biochemistry 9510, University of California, Santa Barbara, CA 93106; and [d]DuPont Central Research and Development, Wilmington, DE 19880

Edited by Allen J. Bard, University of Texas at Austin, Austin, TX, and approved February 10, 2010 (received for review December 1, 2009)

Postdeposition solvent annealing of water-dispersible conducting polymers induces dramatic structural rearrangement and improves electrical conductivities by more than two orders of magnitude. We attain electrical conductivities in excess of 50 S/cm when polyaniline films are exposed to dichloroacetic acid. Subjecting commercially available poly(ethylene dioxythiophene) to the same treatment yields a conductivity as high as 250 S/cm. This process has enabled the wide incorporation of conducting polymers in organic electronics; conducting polymers that are not typically processable can now be deposited from solution and their conductivities subsequently enhanced to practical levels via a simple and straightforward solvent annealing process. The treated conducting polymers are thus promising alternatives for metals as source and drain electrodes in organic thin-film transistors as well as for transparent metal oxide conductors as anodes in organic solar cells and light-emitting diodes.

electrical conductivity | solar cells | thin-film transistors | light-emitting diodes | polyaniline

The promise of organic devices as platforms for lightweight, low-cost, and mechanically flexible plastic electronics has spurred research in conducting polymers (1–6). Though highly conductive (>100 S/cm), these early conjugated systems are frequently insoluble in common solvents, severely restricting their utility in proposed applications. To overcome the intractability of conducting polymers, polymer acids—instead of small-molecule acids—have been used as counterions to maintain charge neutrality in doped poly(ethylene dioxythiophene), PEDOT, or as proton sources for doping polyaniline, PANI, effectively rendering these materials water dispersible. Such enhancement in processability, however, comes at the expense of electrical conductivity, presumably due to additional structural disorder the polymer acid introduces during template polymerization. Polymer acid templated conducting polymers thus frequently exhibit electrical conductivities (<1 S/cm) that are several orders of magnitude lower than those of small-molecule acid doped systems. When these polymers are incorporated as electrodes in organic thin-film transistors (OTFTs) (7, 8), or as anodes in organic solar cells (OSCs) (9, 10) and light-emitting diodes (OLEDs) (11, 12), the bulk resistance of the conducting polymers severely limits device performance.

Exposing conducting polymers to selective reagents can improve electrical conductivities through a process known as secondary doping (13–18). When commercially available PEDOT that is template synthesized with poly(styrene sulfonic acid), PEDOT-PSS, is exposed to sorbitol (16), dimethylsulfoxide (17), or ethylene glycol (18), for example, its electrical conductivity can be improved by an order of magnitude. Despite such reports, the mechanism by which this conductivity enhancement occurs via exposures to seemingly unrelated solvents remains controversial (14–18). Elucidation of the origin of conductivity enhancement is further complicated by the fact that these reagents are highly specific to PEDOT-PSS; exposing water-dispersible, polymer acid templated PANI to these reagents does not improve its conductivity. Although conductivity enhancement has been demonstrated with the secondary doping of small-molecule acid doped PANI with exposure to select solvents (13, 19, 20), there have been no reports to date of postdeposition conductivity enhancement in polymer acid templated PANI.

Starting with PANI that is templated with poly(2-acrylamido-2-methyl-1-propanesulfonic acid), or PANI-PAAMPSA, we have improved its conductivity by more than two orders of magnitude through a simple exposure to dichloroacetic acid (DCA) and we further elucidate the mechanism by which this conductivity improvement occurs. More importantly, this treatment is general and can be applied to other polymer acid templated conducting polymer systems; exposing PEDOT-PSS to DCA results in an electrical conductivity as high as 250 S/cm. When DCA-treated conducting polymers are incorporated as electrodes in OTFTs and as anodes in OSCs and OLEDs, the bulk resistance that plagues devices with untreated conducting polymer electrodes is effectively eliminated. These materials—readily processed from solution—thus make excellent alternatives to costly metals and metal oxide conductors in organic electronics.

Results and Discussion

Fig. 1 shows the electrical and structural characterization of PANI-PAAMPSA before and after DCA treatment. Four-probe measurements on drop-cast PANI-PAAMPSA films yield currents on the order of 10^{-1} mA when a 10 V bias is applied (representative data presented as solid line in Fig. 1*A*; magnified in inset). Given the slope of the current–voltage (*I*–*V*) characteristics and the film dimensions, the conductivity of pristine PANI-PAAMPSA is 0.38 ± 0.05 S/cm; we obtain comparable values via the transmission line method (21, 22). After DCA treatment, applying a 10 V bias across the same films results in current levels that are two orders of magnitude higher (representative data presented as dashed line in Fig. 1*A*). Accordingly, the conductivity increases 110-fold to 40.78 ± 10.17 S/cm. Fig. 1*B* shows the ultraviolet-visible-near infrared (UV-vis-NIR) spectra of PANI-PAAMPSA before (solid line) and after DCA treatment (dashed line). The spectrum of untreated PANI-PAAMPSA film exhibits a broad band that is attributed to the π-π^* transition between 310 and 450 nm and a polaron transition at approximately 800 nm (20, 23). Both absorptions are characteristic of PANI having a compact coil conformation; this spectrum is generally associated with PANI having low conductivities (0.01–1 S/cm) (13, 19). The UV-vis-NIR spectrum of DCA-treated PANI-PAAMPSA shows significant absorption that extends into the NIR region. The

Author contributions: Y.-L.L. designed research; J.E.Y., K.S.L., A.G., J.T., and K.B. performed research; E.D.G., Y.S., and H.M. contributed new reagents/analytic tools; J.E.Y., K.S.L., A.G., and T.-Q.N. analyzed data; and J.E.Y., J.T., T.-Q.N., and Y.-L.L. wrote the paper.

The authors declare no conflict of interest.

This article is a PNAS Direct Submission.

[1]To whom correspondence should be addressed. E-mail: lloo@princeton.edu.

This article contains supporting information online at www.pnas.org/cgi/content/full/0913879107/DCSupplemental.

www.pnas.org/cgi/doi/10.1073/pnas.0913879107

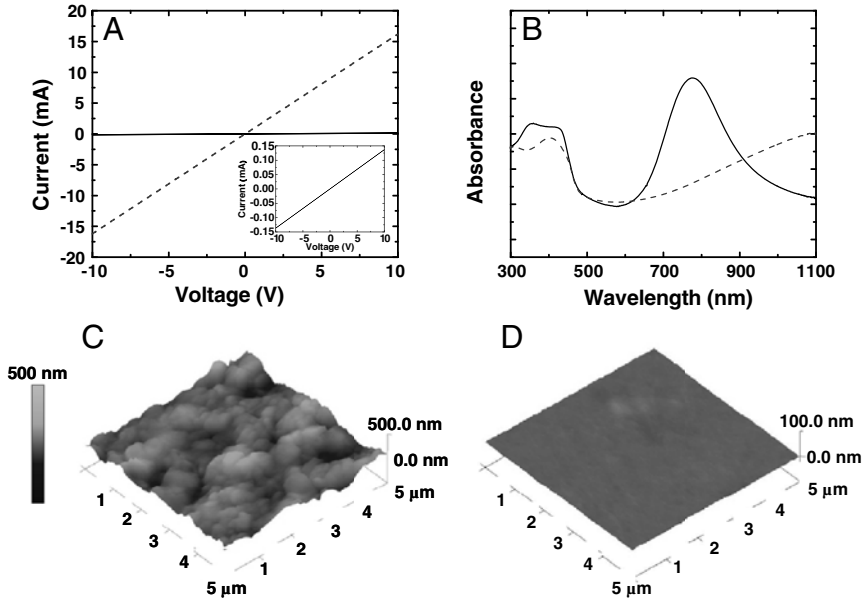

Fig. 1. (*A*) *I–V* characteristics and (*B*) UV-vis-NIR spectra of untreated (solid lines) and DCA-treated (dashed lines) PANI-PAAMPSA. Inset of *A*: *I–V* characteristics of untreated PANI-PAAMPSA. AFM images of (*C*) untreated (rms roughness of ≈60.3 nm) and (*D*) DCA-treated (rms roughness of ≈4.3 nm) PANI-PAAMPSA.

presence of this free-carrier tail has previously been observed in small-molecule acid doped PANI upon secondary doping, and suggests PANI with an extended chain conformation (13, 19). Fig. 1*C* and *D* contain representative atomic force micrographs (AFMs) of PANI-PAAMPSA before and after DCA treatment, respectively. The pristine PANI-PAAMPSA film is rough (rms roughness is 60.3 nm in the 5×5-μm window) and exhibits features that are reminiscent of electrostatically stabilized colloidal particles typical of conducting polymers from template synthesis on polymer acids (22). With DCA treatment, the same film now appears featureless, with an rms roughness of 4.3 nm. Exposing PANI-PAAMPSA to DCA enhances its electrical conductivity; this conductivity improvement is accompanied by dramatic structural rearrangement that traverses multiple length scales.

During template polymerization, PANI-PAAMPSA forms submicron colloidal particles that are electrostatically stabilized by ionic interactions between the $-SO_3^-$ groups of PAAMPSA and the aniline repeat units. When cast as films, the connectivity of these particles limits bulk electrical conductivity (22). Exposing PANI-PAAMPSA films to DCA "dissolves" these PANI-PAAMPSA particles, resulting in a smooth film with high conductivity. To understand the role DCA plays during solvent annealing, we measured the ionization constants (pK_a) of DCA and PAAMPSA (details provided in supplementary information). The pK_a of DCA is 0.70 whereas that of PAAMPSA is 2.29 at 70 °C. Given that DCA is a good solvent for PAAMPSA and its pK_a lower than that of PAAMPSA, exposing the film to DCA must effectively plasticize PANI-PAAMPSA and induce structural rearrangement via disruption of ionic interactions between the $-SO_3^-$ groups of PAAMPSA and the aniline repeat units. During solvent annealing with DCA, the relaxation of particles leads to a more favorable conformation for charge transport. X-ray photoelectron spectroscopy (XPS) experiments on PANI-PAAMPSA films before and after exposure to DCA verify the modulation of ionic interactions in PANI-PAAMPSA (*SI Text*). These experiments also point to the absence of chlorine in the DCA-annealed film, indicating the complete removal of DCA after treatment and disproves DCA-doping of PANI (24) as a source of conductivity improvement.

We carried out additional control experiments by treating PANI-PAAMPSA films with trichloroacetic acid (TCA), DMSO, and hydrochloric acid (HCl). Like DCA, TCA is a good solvent for PAAMPSA and has a pK_a (0.89 at 25 °C) that is lower than PAAMPSA (25); exposing PANI-PAAMPSA to TCA thus induces structural rearrangement and a concurrent increase in electrical conductivity (34.75 ± 6.31 S/cm). DMSO and HCl are negative controls: DMSO is not acidic ($pK_a = 35$ at 25 °C) despite being a good solvent for PAAMPSA, and HCl is a bad solvent for PAAMPSA though it has a low pK_a (−7 at 25 °C). When PANI-PAAMPSA is annealed in DMSO, the conductivity remains unchanged and we do not observe any structural rearrangement, implicating the importance of solvent acidity for this process.

Exposing PANI-PAAMPSA to HCl results in a small increase in its conductivity (1.88 ± 0.26 S/cm). Unlike PANI-PAAMPSA films that are exposed to DCA, however, the AFMs of HCl-treated PANI-PAAMPSA films is not different from that of pristine PANI-PAAMPSA (see *SI Text*); we still observe submicron size particles composing the films. The UV-vis-NIR spectrum of HCl-treated PANI-PAAMPSA is similar to that of untreated PANI-PAAMPSA, indicating that PANI-PAAMPSA retains its compact coil conformation despite exposure to HCl. This increase in conductivity when PANI-PAAMPSA is exposed to HCl is thus not induced by structural rearrangement. When PANI is template synthesized with high molecular weight PAAMPSA, PANI-PAAMPSA is only partially doped due to mass transfer limitations of the polymer acid (21). This 5-fold increase in conductivity of PANI-PAAMPSA is thus attributed to HCl doping of residual imine sites along the PANI backbone (21). Because HCl is a bad solvent for PAAMPSA, it cannot induce the dramatic structural changes or the accompanying conductivity enhancement seen with DCA treatment of PANI-PAAMPSA. Collectively, our control experiments implicate the requirement of a solvent that is a good plasticizer and a stronger acid than the polymer acid for drastic conductivity enhancement.

To evaluate the generality of this treatment, we also solvent annealed PANI-PSS and PEDOT-PSS. With DCA treatment, the conductivity of PANI-PSS increases nearly 250-fold, from 0.17 ± 0.04 S/cm to 42.37 ± 12.49 S/cm. Given that DCA is a good plasticizer for PSS and its pK_a lower than that of PSS ($pK_a = 0.70$ and 1.95, respectively, at 70 °C), solvent annealing with DCA can also relax the electrostatically stabilized PANI-PSS particles that are formed during template polymerization.

Solvent annealing PEDOT-PSS with DCA also results in a dramatic conductivity improvement of 835-fold, from 0.21± 0.05 S/cm to 175.39 ± 59.7 S/cm. Unlike solvent annealing of PANI, however, exposing PEDOT-PSS to DCA causes significant roughening of the conducting polymer film (the rms roughness increases from 0.9 to 2.6 nm; see *SI Text*). A different mechanism must thus be at play when PEDOT-PSS is exposed to DCA. Given that PANI is rendered electrically conductive via proton doping while conductive PEDOT is obtained on oxidative doping, it is not surprising that the origin of conductivity enhancement in these systems is different when exposed to DCA. Furthermore, spin casting PEDOT-PSS results in the formation of a thin insulating PSS overlayer (15, 22, 26). We thus hypothesize that solvent annealing—with DCA being a good solvent for PSS—disrupts this insulating overlayer, effectively enhancing the bulk conductivity of PEDOT-PSS films. In this case, the acidity of the solvent is irrelevant because oxidative doping of PEDOT-PSS is pH independent. Indeed, prior reports indicate that exposing PEDOT-PSS to DMSO (17), ethylene glycol (15), and n-methylpyrrolidone (18)—all good solvents for PSS but none strong acids—can improve its bulk conductivity. Further evidence that conductivity enhancement in PEDOT-PSS arises from the selective surface enhancement of PEDOT stems from XPS and UV-vis-NIR spectroscopy experiments (see *SI Text*), which collectively indicate an increase in PEDOT concentration at the film surface after exposure to DCA without significant change in polymer conformation.

To examine the versatility of DCA-treated conducting polymers, we incorporated PANI-PAAMPSA and PEDOT-PSS as functional components in OTFTs, OSCs, and OLEDs. Fig. 2 contains representative the *I–V* characteristics of bottom-contact OTFTs with untreated and DCA-treated PANI-PAAMPSA as source and drain electrodes and dihexylthiophene anthracene, DHT-ANT (27), as the active layer; the corresponding transfer characteristics are also included. The field-modulated current from the device with untreated PANI-PAAMPSA electrodes suffers from significant hysteresis and we observe severe current crowding at gate voltages beyond −5 V because PANI-PAAMPSA electrodes are resistive. When DCA-treated PANI-PAAMPSA electrodes replace untreated electrodes in these OTFTs, the output currents are at least an order of magnitude higher and the hysteresis is completely eliminated. Further, the transfer characteristics are well behaved, indicating that field modulation of the output current is no longer limited by the bulk resistance of PANI-PAAMPSA electrodes. Replacing pristine electrodes with DCA-treated PANI-PAAMPSA electrodes in OTFTs increases the device mobility from 0.007 ± 0.003 $cm^2/V s$ to 0.07± 0.02 $cm^2/V s$ and the on/off current ratio from 10^3 to 10^5.

When spun cast as thin films on glass substrates, DCA-treated PANI-PAAMPSA (300 nm) and PEDOT-PSS (400 nm) are colored but transparent (Fig. 3*A*). The transmission spectra of these films along with that of indium tin oxide (ITO) coated with 60-nm-thick PEDOT-PSS (to simulate the common buffer layer/ITO combination used in organic optoelectronics) are shown in Fig. 3*B*. At $\lambda = 555$ nm, where the human eye is most sensitive, PEDOT-PSS/ITO has a transmissivity of 84%. DCA-treated PANI-PAAMPSA and PEDOT-PSS transmit 69% and 73%, respectively. The same films exhibit sheet resistances of 2690± 1000 Ω/sq and 280 ± 14 Ω/sq, respectively. While the transmissivities of DCA-treated conducting polymers are lower and the sheet resistances higher than that of PEDOT-PSS/ITO (of order 10 Ω/sq), at a fraction of the cost, these conducting polymers remain attractive alternatives to ITO as transparent anodes in OSCs. To test their viability, we fabricated and tested bulk heterojunction OSCs whose photoactive layer consists of a blend of poly(3-hexylthiophene), P3HT, and [6,6]-phenyl-C61-butyric acid methyl ester, PCBM, in which untreated and DCA-treated

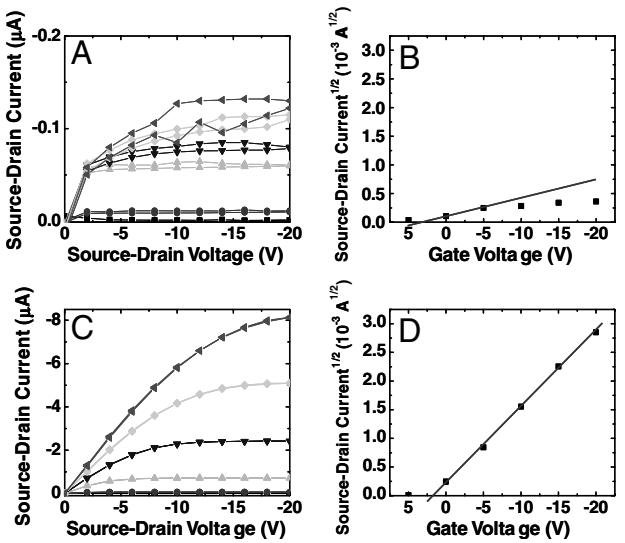

Fig. 2. (*A*) *I–V* characteristics of a bottom-contact DHT-ANT TFT with untreated PANI-PAAMPSA electrodes and (*B*) its corresponding transfer characteristics. The mobility extracted from the slope (solid line) of the transfer characteristics is 0.004 cm^2/V-s. (*C*) *I–V* characteristics of a bottom-contact DHT-ANT TFT with DCA-treated PANI-PAAMPSA electrodes and (*D*) its corresponding transfer characteristics. The mobility extracted from the slope (solid line) of the transfer characteristics is 0.09 cm^2/V-s. The channel dimensions of both devices are $L \cong 100$ μm and $W \cong 1,000$ μm.

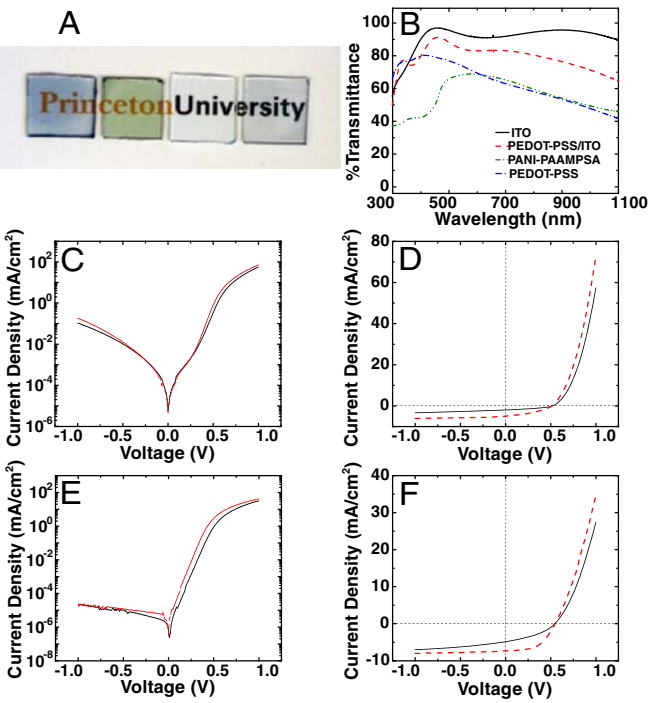

Fig. 3. (*A*) Photographs of (left to right) DCA-treated PEDOT-PSS (400 nm) and PANI-PAAMPSA (300 nm) on glass, ITO (150 nm) on glass, and 60 nm of PEDOT-PSS on ITO/glass; (*B*) corresponding transmission spectra for ITO (solid line), PEDOT-PSS/ITO (dashed line), and DCA-treated PANI-PAAMPSA (dash-dot-dotted line) and PEDOT-PSS (dash-dotted line) films. J-V characteristics of OSCs (*C*) in the dark and (*D*) under illumination (100 mW/cm^2) with untreated (solid line) and DCA-treated (dashed line) PANI-PAAMPSA anodes, and J-V characteristics of OSCs (*E*) in the dark and (*F*) under illumination (100 mW/cm^2) with untreated (solid line) and DCA-treated (dashed line) PEDOT-PSS anodes. The active area in all devices is 0.0625 cm^2. All devices were fabricated and tested under ambient conditions.

conducting polymers replace ITO as anodes. Aluminum was used as cathodes; the devices were constructed and tested in air. Fig. 3 contains the diode characteristics (*C*) and the illuminated photovoltaic characteristics (*D*) of representative devices with untreated and DCA-treated PANI-PAAMPSA anodes. The photovoltaic parameters of these devices, including the series and shunt resistances extracted from J-V characteristics, are summarized in Table 1. Consistent with the fact that the open-circuit voltage (V_{OC}) is, to first order, dictated by the energy levels of the electron donor and acceptor within the photoactive layer (28), it remains at 0.51 V independent of whether the anode is treated with DCA. Replacing untreated PANI-PAAMPSA with DCA-treated PANI-PAAMPSA anodes increases the average short-circuit current density (J_{SC}) from 1.95 ± 0.08 mA/cm^2 to 4.95 ± 0.16 mA/cm^2, effectively increasing the device efficiency from $0.39 \pm 0.05\%$ to $0.97 \pm 0.18\%$. This increase in current density stems from a decrease in series resistance in our device. We also fabricated and tested OSCs with untreated and DCA-treated PEDOT-PSS as anodes. Consistent with OSCs with PANI-PAAMPSA anodes, incorporation of DCA-treated PEDOT-PSS anodes increases the J_{SC} by 1.5-fold compared to devices with pristine PEDOT-PSS anodes. This increase is also attributed to a significant decrease in the series resistance in the device with DCA-treated anode, ultimately resulting in improved diode characteristics when the device is tested in the dark (Fig. 3*E*) and a higher fill factor under illumination (Fig. 3*F*). The V_{OC} in these OSCs is pinned at 0.55 V given that the energetics of the devices with untreated and treated PEDOT-PSS anodes are comparable. The V_{OC} of OSCs with PEDOT-PSS anodes is slightly higher than that of devices with PANI-PAAMPSA anodes, likely due to slight differences in the work function of the two conducting polymers. Devices with DCA-treated PEDOT-PSS anodes have average efficiencies of $2.12 \pm 0.16\%$ when tested in air as opposed to $0.97 \pm 0.14\%$ for devices with untreated PEDOT-PSS anodes. Given that DCA-treated PEDOT-PSS is significantly more conductive compared to DCA-treated PANI-PAAMPSA, it is not surprising that devices comprising DCA-treated PEDOT-PSS consistently outperform those with DCA-treated PANI-PAAMPSA anodes.

Transparent metal oxides are also commonly used in OLEDs. To assess the wide incorporation of DCA-treated conducting polymers in organic electronics, we also examined the performance of OLEDs comprising poly(2-methoxy-5-(2′-ethyl-hexyloxy)-1,4-phenylene vinylene), MEH-PPV (emissive layer), with conducting polymer anodes and barium cathodes for hole and electron injection, respectively. Fig. 4 contains the luminance characteristics of OLEDs with untreated and DCA-treated PANI-PAAMPSA anodes (*A*) as well as those of OLEDs with untreated and DCA-treated PEDOT-PSS anodes (*B*). The device characteristics are detailed in Table 1. Replacing DCA-treated PANI-PAAMPSA anodes for pristine PANI-PAAMPSA anodes significantly reduces the turn-on voltage from 7.6 ± 0.1 V to 2.7 ± 0.1 V. Further, we observe a nearly 10-fold increase (from 2.1 ± 0.6 Cd/m^2 to 22.0 ± 0.7 Cd/m^2) in the maximum lumens

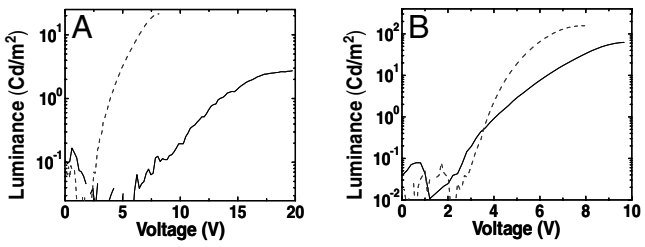

Fig. 4. Luminance characteristics of OLEDs with (*A*) untreated (solid line) and DCA-treated (dashed line) PANI-PAAMPSA anodes, as well as with (*B*) untreated (solid line) and DCA-treated (dashed line) PEDOT-PSS anodes.

when DCA-treated PANI-PAAMPSA anodes are employed in our OLEDs. OLEDs with PEDOT-PSS anodes generally outperform those with PANI-PAAMPSA electrodes. When pristine PEDOT-PSS is incorporated in OLEDs as anodes, we observe a turn-on voltage of 2.8 ± 0.1 V and a maximum lumens of 45.6 ± 17.4 Cd/m^2. Replacing pristine PEDOT-PSS with DCA-treated PEDOT-PSS anodes further increases device parameters; we record a maximum lumens of 334.9 ± 177.3 Cd/m^2 for OLEDs with DCA-treated PEDOT-PSS anodes. None of our devices exhibit the high luminance typical of OLEDs (>1,000 Cd/m^2) because of imbalance charge transport (29, 30) in MEH-PPV where the electron mobility is significantly lower than the hole mobility (31). Nonetheless, the conductivity enhancement in PANI-PAAMPSA and PEDOT-PSS directly impacts the ease with which holes are injected from the anode leading to enhance OLED performance.

Polymer acid templated conducting polymers were developed to overcome the intractability of small-molecule acid doped systems. The gain in processability has frequently come at the expense of conductivity, severely limiting the utility of these materials. With a simple postdeposition solvent annealing treatment that is widely applicable to a broad range of materials, we can dramatically improve the conductivity of water-dispersible conducting polymers; the conductivities achieved through this treatment qualify the treated conducting polymers as practical alternatives to metals and transparent metal oxides that are used as electrodes in organic electronics. As demonstrated, this treatment will enable the broad incorporation of conducting polymers in organic electronic applications. Water-dispersible systems can be deposited and patterned (32), and now their conductivity can be enhanced to practical levels via this postdeposition solvent annealing process.

Materials and Methods

Polymer Synthesis. PANI-PAAMPSA was synthesized according to previously published procedures (21). To synthesize PANI-PSS, we first converted commercially available PSS-Na (Alfa Aesar; $M_w = 500$ kg/mol) to its acidic form via ion exchange. PSS was then used to template synthesize PANI-PSS according published procedures (21).

We dispersed purified PANI-PAAMPSA and PANI-PSS at 5 wt% in deionized water; the dispersion was stirred for 10–14 days before use. PEDOT-PSS dispersion was used as received from H.C. Starck. We first spin coated the conducting polymer dispersions on either Si/SiO_2 or glass substrates at 1,000 rpm. The polymer films were baked at 100 °C for 3 min to remove residual water. We then agitated the films in preheated DCA (Acros Organics, 99 + %) at 100 °C for 3 min. The treated films were then baked at elevated temperatures for 30 min to remove DCA. After DCA treatment, we exposed the films to <10^{-7} torr vacuum for more than 3 h to remove residual DCA prior to any characterization.

Titration Experiments. The ionization constants (pK_a) of DCA and polymer acids were measured via titration with 0.1 M sodium hydroxide at 70 °C. We tracked the pH as 10^{-5} M DCA and 10^{-7} M PAAMPSA and PSS were titrated with sodium hydroxide.

Characterization Techniques and Procedures. The electrical conductivities of conducting polymer films were measured using the four-point probe method (21, 33) with an Agilent 4155C Semiconductor Parameter Analyzer. We measured the thicknesses of the conducting polymer films before and after DCA treatment using a Dektak 3.21 profilometer. AFM images of the conducting polymer films were obtained on a Digital Instrument Nanoscope IIIa. The rms roughness was quantified using NanoScope Software version 7.00b20. UV-vis-NIR spectra of the conducting polymer films on glass substrates were collected using an Agilent 8453 UV-vis-NIR spectrometer. We used a clean glass slide as background. Sample spectra were collected in the wavelength range of 300–1100 nm.

XPS was carried out using a Physical Electronics ESCA 5700 spectrophotometer equipped with a monochromatic Al Kα x-ray source and a hemispherical electron analyzer. All spectra were collected at a base pressure of $\approx 2 \times 10^{-8}$ torr at ambient temperature. High-resolution scans were acquired at 0.1-eV increment with a sweep time of 1,000 ms/eV and 10 energy sweeps for each spectrum. Prior to data analysis, the binding energy

Table 1. Summary of device characteristics for (AOTFTs, OSCs, and OLEDs with untreated and DCA-treated conducting polymer electrodes

Device types	Device characteristics					
Electrodes in OTFTs	*Mobility,* $cm^2/V\,s$				*On/off current ratio*	
PANI-PAAMPSA	0.007 ± 0.003				10^3	
DCA-treated PANI-PAAMPSA	0.07 ± 0.02				10^5	
Anodes in OSCs	J_{sc}, mA/cm^2	V_{oc}, *V*	*Fill factor, FF*	*Efficiency, %*	*Series resistance,* $\Omega\,cm^2$	*Shunt resistance,* $\Omega\,cm^2$
PANI-PAAMPSA	1.95 ± 0.08	0.52 ± 0.01	0.38 ± 0.01	0.39 ± 0.05	5.32 ± 1.72	1440.3 ± 212.35
DCA-treated PANI-PAAMPSA	4.95 ± 0.16	0.51 ± 0.02	0.38 ± 0.02	0.97 ± 0.18	3.93 ± 1.41	1503.5 ± 256.34
PEDOT-PSS	4.59 ± 0.21	0.55 ± 0.01	0.38 ± 0.02	0.97 ± 0.14	8.58 ± 2.51	1652.5 ± 200.21
DCA-treated PEDOT-PSS	7.36 ± 0.14	0.55 ± 0.01	0.52 ± 0.01	2.12 ± 0.16	2.49 ± 0.87	1686.7 ± 214.85
Anodes in OLEDs	*Turn-on voltage, V*				*Maximum luminance,* Cd/m^2	
PANI-PAAMPSA	7.6 ± 0.1				2.1 ± 0.6	
DCA-treated PANI-PAAMPSA	2.7 ± 0.1				22.0 ± 0.7	
PEDOT-PSS	2.8 ± 0.1				45.6 ± 17.4	
DCA-treated PEDOT-PSS	2.9 ± 0.2				334.9 ± 177.3	

Reported averages and standard deviations were extracted from measurements of characteristics of at least three devices.

of the core level C1s peak was set at 284.5 eV to compensate any surface charging effects and all elemental spectra were shifted accordingly. During data fitting, the peak positions and the full widths at half the maximum intensity of the peaks were kept constant; the peak intensities were the only floating parameters. The relative concentration of the individual species was then extracted by comparing the relevant integrated peak intensities.

Device Fabrication and Testing. To fabricate bottom-contact OTFTs, we first defined PANI-PAAMPSA source and drain electrodes on Si/SiO_2 substrates (32). The channel length (*L*) and width (*W*) of our OTFTs are 100 and 1,000 μm, respectively. To fabricate devices with highly conductive PANI-PAAMPSA electrodes, the electrodes were subjected to DCA treatment before the deposition of DHT-ANT (27) via thermal evaporation. Averages and standard deviations were extracted from at least 90 measurements on individual and separate films cast from different batches of conducting polymers.

To fabricate OSCs, we first deposited gold grids on bare glass substrates. PANI-PAAMPSA and PEDOT-PSS aqueous dispersions were spin coated on the predefined gold grids at 1,000 rpm for 1 min to define the anodes. DCA treatment was performed subsequently. P3HT (Merck) and PCBM (Nano-C) was codissolved at 1:0.8 (wt/wt) in chlorobenzene to yield a 2.4 wt% solution and the solution was deposited by spin coating directly on PANI-PAAMPSA (or PEDOT-PSS) anodes at 500 rpm for 1 min resulting in active layers approximately 150-nm thick. We then deposited 100 nm of aluminum by thermal evaporation through a shadow mask to form the cathodes. The active area of our OSCs is 0.0625 cm^2. All devices were fabricated and tested immediately in air.

Conducting polymer anodes for OLEDs were fabricated in an analogous fashion as those fabricated for OSCs. MEH-PPV was then spin coated from a 0.5% wt/vol toluene solution resulting in an 80-nm-thick emissive layer on conducting polymer anodes. The devices were completed by thermal evaporation of cathodes consisting of ~5 nm of barium and 100 nm of aluminum using a shadow mask at a pressure of 10^{-6} torr. Devices were tested with a Keithley 2602 source meter measuring unit and the luminance signal was collected with a Thorlabs photodetector. All OLEDs were fabricated and tested in a nitrogen-filled glovebox.

ACKNOWLEDGMENTS. We gratefully acknowledge funding from the Keck Foundation, the Beckman Foundation, and the National Science Foundation via a CAREER Award to Y.L.L. (DMR0735148) and a grant through Jackson State University and the University of California, Santa Barbara to T.Q.N. (DMR0611539).

1. Winther-Jensen B, Winther-Jensen O, Forsyth M, MacFarlane DR (2008) High rates of oxygen reduction over a vapor phase-polymerized PEDOT electrode. *Science* 321:671–674.
2. Stutzmann N, Friend RH, Sirringhaus H (2003) Self-aligned, vertical-channel, polymer field-effect transistors. *Science* 299:1881–1884.
3. Sirringhaus H, et al. (2000) High-resolution inkjet printing of all-polymer transistor circuits. *Science* 290:2123–2126.
4. Friend RH, et al. (1999) Electroluminescence in conjugated polymers. *Nature* 397:121–128.
5. Kim JY, et al. (2007) Efficient tandem polymer solar cells fabricated by all-solution processing. *Science* 317:222–225.
6. Müller CD, et al. (2003) Multi-colour organic light-emitting displays by solution processing. *Nature* 421:829–833.
7. Lee KS, et al. (2006) High-resolution characterization of pentacene-polyaniline interfaces in thin-film transistors. *Adv Funct Mater* 16:2409–2414.
8. Lim JA, et al. (2006) Solvent effect of inkjet printed source/drain electrodes on electrical properties of polymer thin-film transistors. *Appl Phys Lett* 88:082102.1–3.
9. Na S-I, Kim S-S, Jo J, Kim D-Y (2008) Efficient and flexible ITO-free organic solar cells using highly conductive polymer anodes. *Adv Mater* 20:1–7.
10. Zhang F, Johansson M, Andersson MR, Hummelen JC, Inganas O (2002) Polymer photovoltaic cells with conducting polymer anodes. *Adv Mater* 14:662–665.
11. Kim WH, et al. (2002) Molecular organic light-emitting diodes using highly conducting polymers as anodes. *Appl Phys Lett* 80:3844–3846.
12. Kim WH, et al. (2002) Molecular organic light emitting diodes using highly conductive and transparent polymeric anodes. *Proc SPIE* 4464:85–92.
13. MacDiarmid AG, Epstein AJ (1994) The concept of secondary doping as applied to polyaniline. *Synthetic Met* 65:103–116.
14. Ouyang J, Chu C-W, Chen F-C, Xu Q, Yang Y (2005) High-conductivity poly(3,4-ethylenedioxythiophene):poly(styrene sulfonate) film and its application in polymer optoelectronic devices. *Adv Funct Mater* 15:203–208.
15. Crispin X, et al. (2003) Conductivity, morphology, interfacial chemistry, and stability of poly(3,4-ethylene dioxythiophene)-poly(styrene sulfonate): A photoelectron spectroscopy study. *J Polym Sci Pol Phys* 41:2561–2583.
16. Jonsson SKM, et al. (2003) The effects of solvents on the morphology and sheet resistance in poly(3,4-ethylenedioxythiophene)-polystyrenesulfonic acid (PEDOT-PSS) films. *Synthetic Met* 139:1–10.
17. Kim JY, Jung JH, Lee DE, Joo J (2002) Enhancement of electrical conductivity of poly (3,4-ethylenedioxythiophene)/poly(4-styrenesulfonate) by a change of solvents. *Synthetic Met* 126:311–316.
18. Ouyang J, et al. (2004) On the mechanism of conductivity enhancement in poly(3,4-ethylenedioxythiophene):poly(styrene sulfonate) film through solvent treatment. *Polymer* 45:8443–8450.
19. MacDiarmid AG, Epstein AJ (1995) Secondary doping in polyaniline. *Synthetic Met* 69:85–92.
20. Xia YN, Wiesinger JM, MacDiarmid AG, Epstein AJ (1995) Camphorsulfonic acid fully doped polyaniline emeraldine salt: Conformations in different solvents studied by an ultraviolet/visible/near-Infrared spectroscopic method. *Chem Mater* 7:443–445.
21. Yoo JE, et al. (2007) Improving the electrical conductivity of polymer acid-doped polyaniline by controlling the template molecular weight. *J Mater Chem* 17:1268–1275.
22. Yoo JE, et al. (2009) Polymer conductivity through particle connectivity. *Chem Mater* 21:1948–1954.
23. Tarver J, Yoo JE, Dennes T, Schwartz J, Loo Y-L (2009) Polymer acid doped polyaniline is electrochemically stable beyond pH 9. *Chem Mater* 21:280–286.
24. Gmati F, Fattoum A, Bohli N, Dhaoui W, Mohamed AB (2007) Comparative studies of the structure, morphology and electrical conductivity of polyaniline weakly doped with chlorocarboxylic acids. *J Phys—Condens Mat* 19:326203.1–3.
25. Trivedi D (1996) *Handbook of Organic Conductive Molecules and Polymers: Vol 2 Conductive Polymers: Synthesis and Electrical Properties*, ed HS Nalwa (Wiley, New York), pp 506–572.
26. Hwang J, Amy F, Kahn A (2006) Spectroscopic study on sputtered PEDOT · PSS: Role of surface PSS layer. *Org Electron* 7:387–396.
27. Meng H, et al. (2005) High-performance, stable organic thin-film field-effect transistors based on bis-5′-alkylthiophen-2′-yl-2,6-anthracene semiconductors. *J Am Chem Soc* 127:2406–2407.

28. Malliaras GG, Salem JR, Brock PJ, Scott JC (1998) Photovoltaic measurement of the built-in potential in organic light emitting diodes and photodiodes. *J Appl Phys* 84:1583–1587.
29. Crone BK, Davids PS, Campbell IH, Smith DL (1998) Device model investigation of single layer organic light emitting diodes. *J Appl Phys* 84:833–842.
30. Albercht U, Bässler H (1995) Efficiency of charge recombination in organic light emitting diodes. *Chem Phys* 199:207–214.
31. Bozano L, Scott JC, Malliaras GC, Brook PJ, Carter SA (1999) Temperature- and field-dependent electron and hole mobilities in polymer light-emitting diodes. *Appl Phys Lett* 74:1132–1134.
32. Lee KS, Blanchet GB, Gao F, Loo Y-L (2005) Direct patterning of conductive water-soluble polyaniline for thin-film organic electronics. *Appl Phys Lett* 86:074102.1–3.
33. Yoo JE, Bucholz TL, Jung S, Loo Y-L (2008) Narrowing the size distribution of the polymer acid improves PANI conductivity. *J Mater Chem* 18:3129–3135.